

continuous double helix of 12 base pairs out of helix *a* and helix *e* (Fig. 2B). This can be done in all sequenced tRNA's, leaving a break in only one chain of the double helix where the chains turn out to go to helix *b* and the variable arm *d*. This break is easily constructed through rotation about sugar to phosphate bonds without distortion of the main helix. Helical segments *b* and *c* are then placed parallel to the main helix fitting into the large groove of the main helix, with a rotation of 180° between parallel helices. The anticodon arm (helix *c*) is placed at the helix *e* end with the anticodon in the Fuller-Hodgson conformation (8) at the extremity of the molecule. This helix can be made coaxial with the main helix by keeping the region of overlap to one base pair or less. When this is done, helix *b* can be moved as far out as 10 Å from the main helix without seriously altering the shoulder region of the scattering curve, but the agreement between the observed and calculated scattering curves is best when helix *b* is placed at an axial separation of about 4.5 Å. This helix is placed in the groove of the helix *e* section of the main helix, situated near the break in the main helix, with the dihydrouridine loop of helix *b* extending in the direction of the CCA hydroxyl end. The shortest distance between phosphates of neighboring helical segments is about 5.5 Å, which might require a divalent cation for stability. This would agree with the findings of Lindahl, Adams, and Fresco (9) that tRNA in the native conformation requires a small number of site-bound divalent cations.

In addition to utilizing tRNA sequence similarities and to matching the experimental x-ray data, the model also agrees with much of the chemical evidence available. The chemically unreactive TψC loop of helix *e* is the least exposed loop, fitting into the groove of helix *c*. Although the small-angle x-ray studies do not warrant placing many restrictions on the unpaired loop regions, it is possible to achieve considerable base-stacking in these regions. The 12 base-pair helix forms a rigid stem on which the remainder of the molecule is folded, and the distance between the anticodon and the CCA-hydroxyl end is constant except for movement of the last four nucleotides of the CCA-hydroxyl end. The anticodon arm, helix *c*, is exposed and free to interact with mRNA in agreement with the evidence of Rudland and Dube (10). A molecule of this size and shape

will fit the unit-cell packing requirements found in crystallographic studies and is consistent with the projected electron density for crystals of *E. coli* tRNA^{Leu} and yeast tRNA^{fMet} (11).

Our model has two important features. (i) Based on the absence, in all sequenced tRNA's, of any unpaired bases between the helical regions *a* and *e*, we have made one continuous helix of 12 base pairs. (ii) Based on small-angle x-ray scattering studies, we have placed the anticodon helix *c* approximately coaxial with the main helix, and the axis of helix *b* at a separation of about 5 Å from it, giving a molecule of dimensions 25 by 35 by 85 Å.

PETER G. CONNORS

MINDAUGAS LABANAUSKAS

Laboratory of Biophysics,
University of Wisconsin,
Madison 53706

W. W. BEEMAN

Department of Physics and
Laboratory of Biophysics,
University of Wisconsin

References and Notes

- Abbreviations are: tRNA, transfer ribonucleic acid; mRNA, messenger RNA; Ala, alanine; fMet, formylmethionine; Tyr, tyrosine; Phe, phenylalanine; A, adenine; C, cytosine; G, guanine; U, uracil; ψ, pseudouracil; T, ribothymidine; poly C, poly cytidylic acid; poly G, poly guanylic acid; and tris, tris(hydroxymethyl)aminomethane.
- H. N. Ritland, P. Kaesberg, W. W. Beeman, *J. Appl. Phys.* **21**, 838 (1950).
- J. A. Lake and W. W. Beeman, *J. Mol. Biol.* **31**, 115 (1968).
- W. R. Krigbaum and R. W. Godwin, *Macromolecules* **1**, 375 (1968).
- S. Arnott, M. H. F. Wilkins, W. Fuller, R. Langridge, *J. Mol. Biol.* **27**, 535 (1967).
- R. Langridge, D. A. Marvin, W. E. Seeds, H. R. Wilson, C. W. Hooper, M. H. F. Wilkins, L. D. Hamilton, *ibid.* **2**, 38 (1960).
- F. Cramer, H. Doepner, F. v. d. Haar, E. Schlimme, H. Seidel, *Proc. Nat. Acad. Sci. U.S.A.* **61**, 1385 (1968).
- W. Fuller and A. Hodgson, *Nature* **215**, 817 (1967).
- T. Lindahl, A. Adams, J. R. Fresco, *Proc. Nat. Acad. Sci. U.S.A.* **55**, 941 (1966).
- P. S. Rudland and S. K. Dube, *J. Mol. Biol.* **43**, 273 (1969).
- M. Labanauskas, P. G. Connors, J. D. Young, R. M. Bock, J. W. Anderegg, W. W. Beeman, *Science*, this issue.
- Supported by NIH research and training grants. We thank Oak Ridge National Laboratories for purified *E. coli* tRNA^{Phe}. We thank U. L. RajBhandary for samples of yeast tRNA^{fMet}, and J. W. Anderegg for advice and assistance.

2 September 1969

Structural Studies on Transfer RNA: Preliminary Crystallographic Analysis

Abstract. *Single-crystal diffraction patterns from Escherichia coli leucine tRNA and yeast formylmethionine tRNA show a tetragonal lattice for the former, with a = 46 Å and c = 137 Å, and a hexagonal lattice for the latter, with a = 115 Å and c = 137 Å. Initial analysis suggests a molecule with a long, double helix parallel to the c-axis for both crystals.*

We present a preliminary analysis of x-ray data collected from crystals of tRNA^{fMet} from yeast and tRNA^{Leu} from *Escherichia coli*. Techniques for crystal growth are discussed in an accompanying report (1). Precession photographs from both crystals are shown in Fig. 1. The space group of the tRNA^{fMet} crystals is *P*₆₂₂ (or *P*₆₄₂₂) with unit cell dimensions *a* = 115 Å and *c* = 137 Å. There are 12 molecules in the unit cell and one molecule per asymmetric unit. The space group of the tRNA^{Leu} crystals is *P*₄₁ (or *P*₄₃) with cell dimensions *a* = 46 Å and *c* = 137 Å. There are four molecules per unit cell and one molecule per asymmetric unit. The resolution of the present data is 10 or 12 Å. The analysis employs model building and Patterson synthesis of the intensities. We discuss here the electron density projected into the basal plane. Only the *F*(*hk*0) are involved.

Based on both chemical and physical evidence several models for tRNA have

been proposed (2–4). Most models, and in particular the one we use (3), suggest a prolate asymmetric molecule with the double-helical regions parallel to the long axis. Such a molecule, properly placed in the unit cell with the helix axes parallel to the *c*-axis, gives excellent agreement with the observed Patterson. The electron density projected into the basal plane is centrosymmetric and the *F*(*hk*0) phases must be zero or π. These phases were calculated from a partial model and with the observed intensities give an electron density map that was used as a guide for the arrangement of the rest of the molecule. The results suggest a molecule containing a long double-helical region around which the rest of the molecule is rather compactly folded. Most of our analysis is on tRNA^{Leu}, but the same model gives good agreement with the data on tRNA^{fMet}.

Figure 2a shows the Patterson synthesis of the experimental intensities of the centrosymmetric *hk*0 plane of the

reciprocal lattice of crystals of tRNA^{Leu} from *E. coli*. Seventeen independent intensities were used. They were corrected for the Lorentz polarization factor and by a temperature factor which increased the intensity of the high order spots, relative to the lowest order, by about 50 percent. An accurate determination of the temperature factor is difficult because of the small number of spots, but it is probably large. Patterson calculations with several different temperature factors showed the same distinctive features. These are the two peaks of high vector density which appear as eight in the figure because of the fourfold symmetry of the projection.

Our model for tRNA is described in an accompanying paper (3). Its principal feature is a long, continuous segment of double helix containing 12 base pairs. Using only the 12 base pair helix (5) as our symmetric unit and assuming that the long axis is parallel to the *c*-axis, we attempted first to locate the helix in the unit cell. An effective number of scattering electrons was assigned to the center of charge of each phosphate, sugar, and base (3). A quadrant of the base plane of the unit cell of tRNA^{Leu} was covered with a square net of 100 points spaced 2.3 Å apart. With the helix axis placed successively at each of these points, the structure amplitude $|F(hk0)|_{\text{calc}}$ for the 17 observed spots were calculated with a Univac 1108 computer and the residuals

$$R = \sum ||F_{\text{obs}}| - |F_{\text{calc}}|| / \sum |F_{\text{obs}}|$$

were evaluated. The net of residuals showed several minimums. At each of these, a Patterson was computed from the calculated structure amplitudes and compared to the observed Patterson. At only one position was the agreement encouraging. The residual at this net point was $R = 0.6$. We next added the remaining double-helical regions to the molecule, assuming their axes to be parallel to the main helix axis. The various parts of the molecule are shown by Connors *et al.* (figure 2, A and B, in 3). The two regions added to the long helix are the stem of the anticodon arm (c) containing five nucleotide pairs and the stem of the dihydrouracil arm (b) for which we used four nucleotide pairs.

We then varied the following parameters on the computer: (i) the position of the main helix axis near the minimum already determined; (ii) separation of the axis of each of the short helices from the axis of the long helix; (iii) the angle between the radial vectors

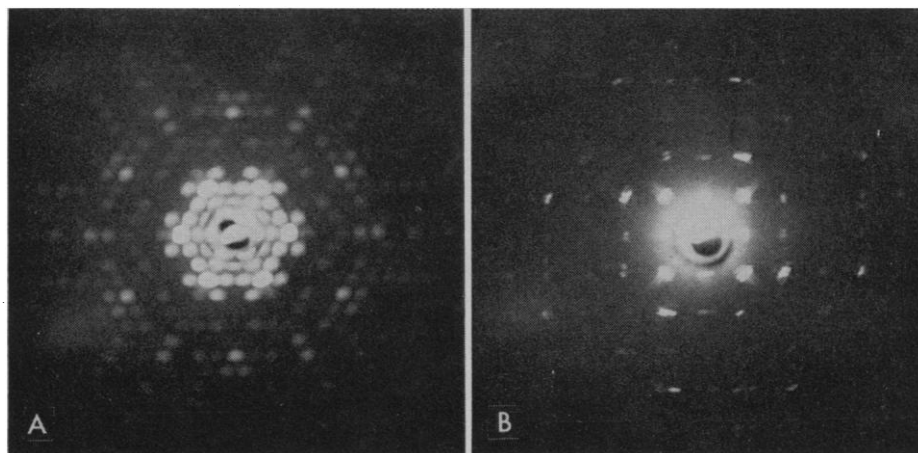


Fig. 1. X-ray precession photographs of (A) the $hk0$ reflections from a crystal of tRNA^{Met} from yeast, and (B) the $hk0$ reflections from a crystal of tRNA^{Leu} from *E. coli*. The spot doubling in (B) is due to twinning. The photographs were taken on a Supper precession camera, with CuK α filtered radiation and a precession angle of 10°.

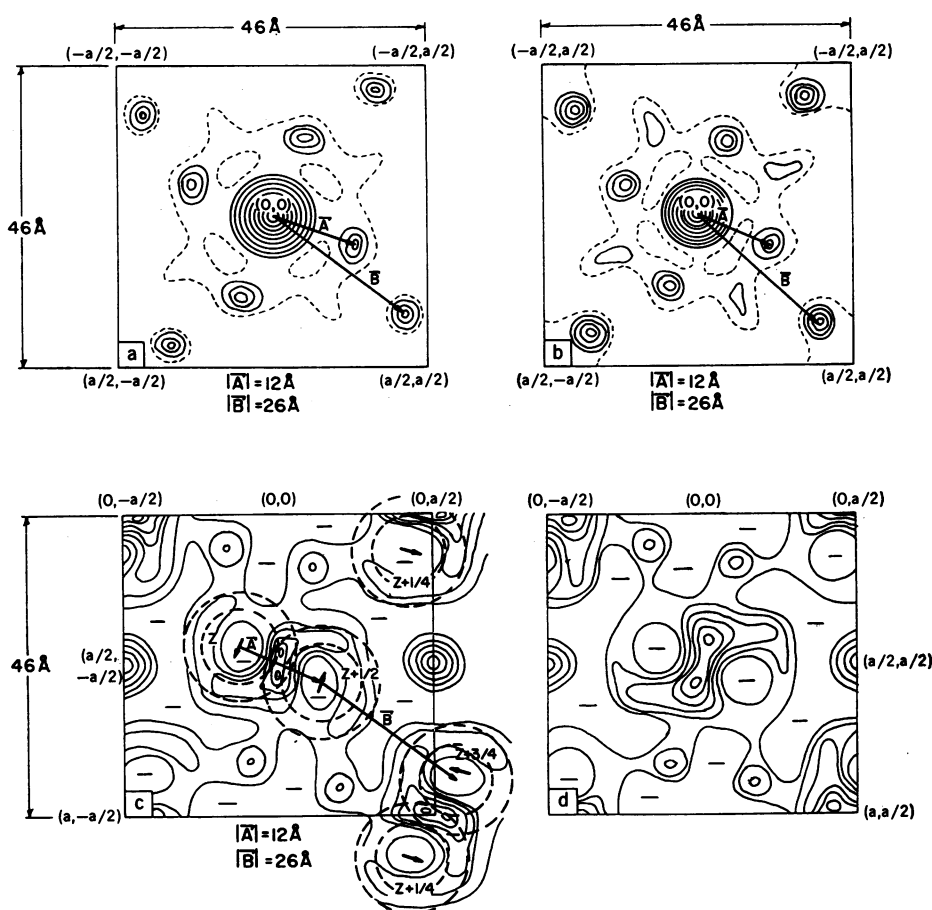


Fig. 2. (a) The Patterson synthesis of the experimental $hk0$ intensities from a crystal of tRNA^{Leu} from *E. coli*. (b) The Patterson synthesis of the calculated $hk0$ intensities from a model of the complete tRNA molecule. (c) The projected electron density in the unit cell of tRNA^{Leu} derived from the model used in (b) by first calculating from the model the structure amplitudes and phases of the observed reflections and, from these, calculating the projected electron density. The $F(0,0,0)$ was not included, and the contours are drawn for every 10 percent above 50 percent of the maximum electron density in the cell. Areas in the cell with less than 50 percent of the maximum electron density are labeled with a minus sign. The long helix of the model is shown as two concentric dotted rings, one at the radius of phosphate, and the other at the radius of the center of charge of an average base. (d) The projected electron density map of the cell of tRNA^{Leu}. The experimental structure factors were used with the phases from the partial model. The resolution is 12 Å. In both (c) and (d), the charge density at $(a/2, a/2)$ is due to the fourfold overlap of a loop.

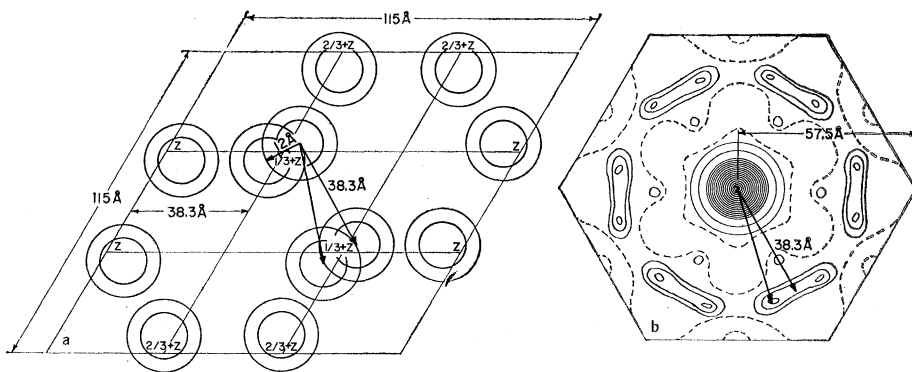


Fig. 3. (a) An arrangement of helices in the unit cell of $tRNA^{fMet}$ which will account for the Patterson synthesis (b) of the experimental ($hk0$) reflections.

from the two short helices to the main helix; and (iv) the rotational orientation of the model in the unit cell. The search through each of the variables was done separately. Each of the optimizations revealed a fairly sharp minimum in R and no great interaction of one optimization with another. The optimized main helix axis location was within 0.5 Å of the position determined in the first search of the net. The residual obtained with the 21 nucleotide pair model was $R = 0.32$, and the agreement of the calculated and observed Pattersons was also improved.

This model included slightly more than half of the nucleotides of the entire molecule. The $R = 0.32$ seemed good enough to justify the calculation of phases. These were assigned to the experimental structure amplitudes, and the projected electron density was computed (Fig. 2d). The dominant features are the rings of charge surrounding the positions of the long helix axes of the model. The rest of the molecule was then added with the least possible alteration of the charge density distribution of Fig. 2d. This can be achieved reasonably well with the model previously described (3) in which the helices of the CCA arm (a) and T ψ CG arm (e) form a continuous 12 base pair double helix. Below this at the T ψ CG end, and coaxial with it, the anticodon arm (c) is placed in the Fuller-Hodgson configuration (6). The crystallography demands a somewhat more asymmetric cross section than was used in (3). We place the dihydrouracil arm (b) about 8 Å from the main helix axis rather than 4 or 5 Å. The complete molecule gives the same phases as those calculated from the 21 nucleotide pair partial model. The Patterson calculated from the complete model is shown in

Fig. 2b, and the electron density at a resolution of 12 Å is in Fig. 2c. The residual is $R = 0.24$.

The most interesting result of the analysis is the evidence for a long double helix parallel to the c -axis. We emphasize that this evidence is quite convincing. The experimental Patterson projection shows peaks which are sharp, circular, and centered at vectors which represent the distances between neighboring molecules. There are two classes of neighboring molecules which, because of the lattice symmetry, are related by rotations of 90° and 180° in the plane of projection. The fact that the Patterson peaks arising from both classes of vectors are similar, sharp, and circular, suggests that at this resolution the molecule's projected electron density is likely to be nearly circular. To check the model dependence of our results, the base plane of the unit cell was searched by use of one turn of a DNA B helix instead of the RNA helix. The residual showed no significant minimums and no sharp Patterson peaks were observed corresponding to translational vectors between molecules. The principal difference in the axial projections of the two helices is the existence of a much higher charge density near the helix axis in the DNA. One expects the translation of a ring of charge to give a Patterson more strongly peaked about the translation vector than does the translation of a disc of charge.

Finally, we point out that if the molecule is in fact 80 or 85 Å long then the pairs whose projections are about 12 Å apart have some end-to-end overlap along the c -axis. The crystal structure is essentially a side-by-side array of chains of overlapping molecules.

Figure 3a shows an arrangement of

helices in the unit cell of $tRNA^{fMet}$ which will account for the peaks in the Patterson synthesis (Fig. 3b) of the experimental $hk0$ reflections. A model similar to that used for $tRNA^{Leu}$ gives a Patterson in excellent agreement with experiment. The residual is 0.27. The pairs of helices are separated by 12 Å just as in the case of $tRNA^{Leu}$. An end-to-end chaining is possible, but, because in $tRNA^{fMet}$ there are dyad axes perpendicular to c , alternate molecules along the chain must be inverted. In $tRNA^{Leu}$ they all point in the same direction.

The model we have used meets the demands of the x-ray data in a natural and straightforward way, but other arrangements of the arms are no doubt possible which give a continuous double helix and compact packing of the rest of the molecule.

MINDAUGAS LABANAUSKAS
PETER G. CONNORS

Laboratory of Biophysics, University
of Wisconsin, Madison 53706

JAMES D. YOUNG, ROBERT M. BOCK
Department of Biochemistry and
Laboratory of Molecular Biology,
University of Wisconsin

J. W. ANDEREGG, W. W. BEEMAN
Department of Physics and Laboratory
of Biophysics, University of Wisconsin

References and Notes

1. J. D. Young, R. M. Bock, S. Nishimura, H. Ishikura, Y. Yamada, U. L. RajBhandary, M. Labanauskas, P. G. Connors, *Science*, this issue.
2. J. A. Lake and W. W. Beeman, *J. Mol. Biol.* **31**, 115 (1968).
3. P. G. Connors, M. Labanauskas, W. W. Beeman, *Science*, this issue.
4. F. Cramer, H. Doepner, F. v. d. Haar, E. Schlimme, H. Seidel, *Proc. Nat. Acad. Sci. U.S.A.* **61**, 1385 (1968).
5. S. Arnott, M. H. F. Wilkins, W. Fuller, R. Langridge, *J. Mol. Biol.* **27**, 535 (1967).
6. W. Fuller and A. Hodgson, *Nature* **215**, 817 (1967).
7. We thank NIH and NSF for financial support from research and training grants and Professor L. Dahl and his group for advice and discussion.

2 September 1969

Physalia Nematocysts: Utilized by Mollusks for Defense

Abstract. *Nudibranchs* Glaucus and *Glaucilla store* and utilize for their own defense the nematocysts of the venomous siphonophore *Physalia*.

During early 1968, bathers in the sea at Port Stephens, New South Wales, Australia, were being unpleasantly